

## Seasonal Variations of Sea Surface Height in the Gulf Stream Region\*

KATHRYN A. KELLY,<sup>+</sup> SANDIPA SINGH, AND RUI XIN HUANG

*Department of Physical Oceanography, Woods Hole Oceanographic Institution, Woods Hole, Massachusetts*

(Manuscript received 2 October 1996, in final form 12 March 1998)

### ABSTRACT

Based on more than four years of altimetric sea surface height (SSH) data, the Gulf Stream shows distinct seasonal variations in surface transport and latitudinal position, with a seasonal range in the SSH difference across the Gulf Stream of 0.14 m and a seasonal range in position of 0.42° lat. The seasonal variations are most pronounced west (upstream) of about 63°W, near the Gulf Stream's warm core. The changes in the SSH difference across the Gulf Stream are successfully modeled as a steric response to ECMWF heat fluxes, after removing the large SSH variations due to seasonal position changes of the Gulf Stream. A phase shift between predicted and observed SSH changes in the Gulf Stream suggests that advection may be important in the seasonal heat budget. Consistent with the interpretation of SSH variations as steric, comparisons with hydrographic data suggest that the fall maximum SSH difference is from the upper 250 m of the water column. The maximum volume transport is in the spring. Zonally averaged indices are used to quantify seasonal changes in the Gulf Stream, which are analogous to changes in the atmospheric jet stream.

### 1. Introduction

Sea surface height (SSH), as measured by a radar altimeter, contains the signature of several ocean processes, including the steric response to the seasonal heating cycle and changes in ocean circulation, both baroclinic and barotropic. Changes in both the ocean's heat storage and the large-scale circulation are important to understanding climate issues; however, it is necessary to distinguish between the two processes in SSH observations. An increase in the transport of the Gulf Stream may signal an increase in the deep-water formation rate at high latitudes. Coupled ocean-atmosphere models suggest that changes in the meridional overturning circulation of the North Atlantic require changes in the Gulf Stream transport (e.g., Delworth et al. 1993). If changes in upper-ocean circulation can be inferred from altimetric SSH, changes in the overturning circulation could be monitored by satellite. On time-scales of weeks, comparisons of altimetric data with

inverted echo sounders suggest that the SSH fluctuations do reflect changes in upper-layer transport (Teague and Hallock 1990; Kelly and Watts 1994; Hallock and Teague 1993). However, seasonal SSH and even inter-annual variations may be dominated by the steric response to seasonal heating.

SSH maps can be interpreted in terms of circulation because the ocean is approximately in geostrophic balance, and the SSH  $\eta$  (relative to the earth's gravitational geoid) gives the surface pressure,  $p' = \rho g \eta$ . Gradients of SSH are related to geostrophic velocity  $\mathbf{u}_g$  at the ocean surface by

$$f\mathbf{k} \times \mathbf{u}_g = -g\nabla\eta, \quad (1)$$

where  $f$  is the Coriolis parameter. A useful quantity in describing the current fluctuations is the SSH difference across the current (surface transport), which is the integral of (one component of) the geostrophic velocity

$$\Delta\eta = \frac{f}{g} \int_y u_g(y') dy', \quad (2)$$

where  $y$  is a line across the Gulf Stream. This quantity is insensitive to the orientation of  $y$  relative to the current direction. To infer volume transport from surface transport, it is necessary to know the vertical structure of the current. In a barotropic ocean, for example,  $\Delta\eta$  would be proportional to the total transport of the current system, or in a system characterized by one active upper layer and a quiescent lower layer, it would be proportional to the transport of the upper layer.

Seasonal heating produces changes in SSH,  $\eta_{\text{steric}}$ , due

\* Woods Hole Oceanographic Institution Contribution Number 9367.

<sup>+</sup> Current affiliation: Applied Physics Laboratory, University of Washington, Seattle, Washington.

*Corresponding author address:* Dr. Kathryn A. Kelly, Applied Physics Laboratory, College of Ocean and Fishery Sciences, University of Washington, 1013 N.E. 40th Street, Seattle, WA 98105-6698.

E-mail: [kkelly@apl.washington.edu](mailto:kkelly@apl.washington.edu)

to the thermal expansion or contraction of the water column, given by

$$\eta_{\text{steric}} = \int_{-h_m}^0 \alpha_T T'_m dz, \quad (3)$$

where  $T'_m$  is the temperature anomaly,  $h_m$  is the depth to which the anomaly penetrates, and  $\alpha_T = -\rho_0^{-1} \partial \rho / \partial T_m$  is the coefficient of thermal expansion. Spatial gradients in  $\eta_{\text{steric}}$  will give rise to geostrophic currents as in (1), but these currents will be confined to the region above the shallow seasonal thermocline (Gill and Niiler 1973). When the dominant source of SSH fluctuations is seasonal heating, then the surface transport anomaly  $\Delta \eta'$  is more logically interpreted as a heat content anomaly than as a volume transport anomaly.

There have been numerous studies of altimetric SSH in an attempt to characterize the seasonal surface transport of western boundary currents. Studies using data from the Geosat altimeter in both the Gulf Stream and the Kuroshio Extension showed that the maximum in SSH difference occurs in the fall (Tai 1990; Zlotnicki 1991; Kelly 1991; Qiu et al. 1991). Recent studies of surface transport using the TOPEX/Poseidon data (Qiu 1995; Wang and Koblinsky 1995), including the analysis presented here, show a fall surface transport maximum. Because hydrographic data show a spring or early summer volume transport maximum (Worthington 1976; Sato and Rossby 1995), seasonal heating has been suspected of creating the fall surface transport maximum. Seasonal heating causes SSH variations of the right magnitude, but the maximum in SSH difference across the Gulf Stream requires that the regions north and south of the Gulf Stream front have seasonal steric responses that differ by more than 0.1 m. Using the Levitus (1982) data, Zlotnicki (1991) suggested that the seasonal cycle in steric height difference was too small by a factor of 2 to explain the Geosat SSH difference. Using the newer version of the Levitus data (Levitus and Boyer 1994), Wang and Koblinsky (1996) showed that the seasonal steric height variations were consistent with seasonal variations in TOPEX/Poseidon SSH in the region of Gulf Stream recirculation. However, based on a buoyancy budget using heat fluxes from the European Centre for Medium-Range Weather Forecasts (ECMWF), they concluded that the heat flux gradients over the Gulf Stream were 2–3 times too small to explain the observed SSH gradients. Here we show that the inconsistency with the ECMWF heat flux is primarily the result of neglecting the SSH variations due to the north–south seasonal Gulf Stream position migration.

There are other low-frequency variations in the Gulf Stream besides the seasonal surface transport (Fig. 1), some of which are similar to those in the atmospheric jet stream. A comparison of SSH from August 1993 (Fig. 1a) and April 1994 (Fig. 1b) shows a decrease in the SSH south of the Gulf Stream and a change from a straight Gulf Stream jet to one with large meanders,

particularly west of about 60°W. The most robust seasonal variation is large-scale position changes: the four years of altimeter data shown here are consistent with analyses of seven years of AVHRR data by Lee and Cornillon (1995) and with previous analyses summarized by Tracey and Watts (1986), showing the most northerly position of the Gulf Stream occurs in the fall. In addition, Kelly (1991) and Qiu et al. (1991) pointed out that more northerly positions of the western boundary current are associated with larger surface transport.

These Gulf Stream fluctuations are reminiscent of changes observed in the atmospheric jet stream. Namias (1950) described the “zonal index cycle” in which the jet stream transitions in late winter or early spring from a northerly straight path with a large eastward velocity (high index) to a more southerly, convoluted path with accompanying cyclones and weak eastward velocity (low index). The zonal index, defined as the zonally averaged eastward velocity in a fixed latitude range, was first introduced by Rossby (1939) and was widely used in synoptic studies of the atmospheric circulation in the 1950s and 1960s. Namias argued that changes in the index cycle were tied to the seasonal heating cycle and that the abrupt change from a high index to a low index in the early spring corresponded to a release of the reservoir of cold air from winter cooling, which was confined to northern latitudes by the strong jet stream.

To quantify the seasonal changes in the SSH, we define several zonally averaged indices. To understand the vertical structure of seasonal variations, we compare the observed SSH variations with dynamic height derived from hydrographic data. Finally, we estimate the effects of seasonal heating on the SSH difference across the Gulf Stream using the net surface heat flux, and discuss some implications of the seasonal heating cycle. The processing of the data fields used in this analysis is described in section 2. Maps of total SSH from the TOPEX/Poseidon altimeter were made by adding the SSH anomaly to a mean SSH (Fig. 2), which is also discussed in section 2. The analyses of the data fields are presented in section 3, followed by a discussion of the results in section 4 and conclusions in section 5.

## 2. Data fields

Collinear height profiles from the TOPEX/Poseidon altimeters [the Archiving Validation and Interpretation of Satellite Oceanographic data (AVISO) Merged Geophysical Data Record] cycles 4 through 80 (October 1992–November 1994) were processed using programs described in Caruso et al. (1990) to obtain profiles of residual SSH. Cycles 1 through 3 were discarded because of poor data quality. All of the suggested corrections from the CD-ROMs were applied and no orbit correction was made. The tidal correction was that of Cartwright and Ray (Ray et al. 1994). Collinear SSH was first averaged in time using a boxcar filter width of 60 days. The temporally averaged values were then spa-

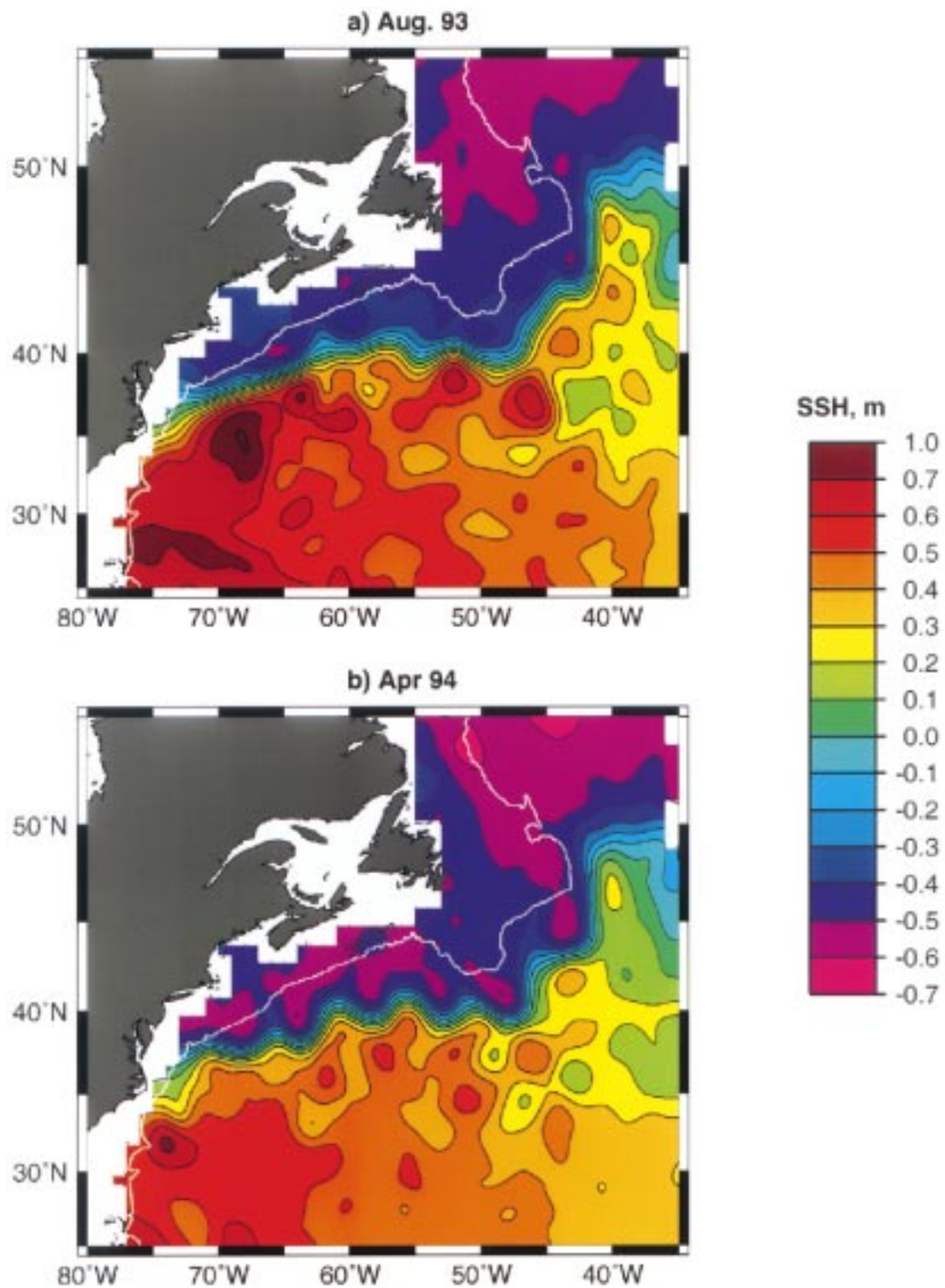


FIG. 1. Sea surface height (SSH) maps for the Gulf Stream region from TOPEX/Poseidon altimeter data. Monthly maps of total SSH for (a) Aug 1993 and (b) Apr 1994, showing a relatively straight path (a) with a large SSH difference across the Gulf Stream and a meandering path (b) with a small SSH difference. The straight path also corresponds to a more northerly position.

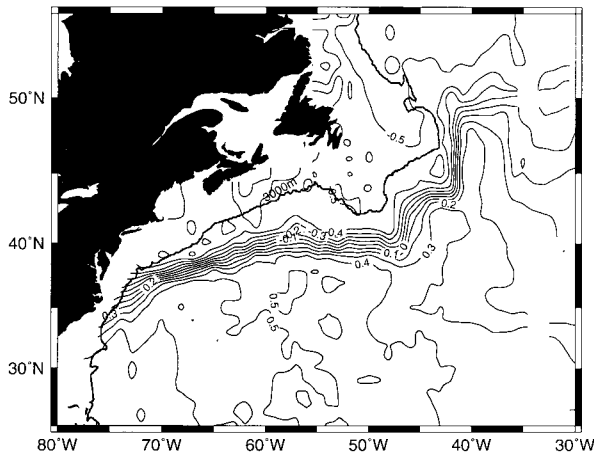


FIG. 2. Mean sea surface height. A mean field was constructed by combining dynamic height from historical hydrographic data with the mean from a jet model applied to altimetric data. Units are meters.

tially interpolated to a  $1^\circ$  grid to produce monthly SSH anomaly maps. The spatial interpolation was done using a two-dimensional biharmonic spline (Sandwell 1987), which adjusts the spline nodes to give better resolution where there are more data, but does not ring in data-sparse regions. The uneven spatial resolution results in a more accurate measure of the SSH difference across the Gulf Stream, but inhomogeneous SSH statistics. In the analyses described here zonal averaging minimized the effect of this inhomogeneity. An estimate of the mean SSH was added to each anomaly map to obtain a total SSH field.

Hydrographic data from the Lozier–Owens–Curry (Lozier et al. 1996, hereafter LOC) hydrographic database (HydroBase) were used to compute climatological estimates of dynamic height. The LOC database contains an extensive set of historical profiles and has the unique quality that quantities are averaged on isopycnal surfaces, rather than on level surfaces, to minimize the smearing out of water properties in an unphysical manner.

The mean SSH (Fig. 2) was constructed using a combination of mean SSH from the Kelly–Gille–Qiu jet model (Kelly and Gille 1990; Qiu et al. 1991) and mean dynamic topography (0/2000 m), as described in Singh and Kelly (1997). Using the LOC HydroBase data and tools, the mean dynamic height was calculated from densities computed by first averaging pressure, temperature, and salinity on density surfaces (Curry 1996). Near the eastward flowing Gulf Stream the mean SSH synthesized from the altimeter data was used; far from the jet and east of  $40^\circ\text{W}$ , the mean dynamic topography was used. To account for the recirculation gyres, which were not modeled in the mean SSH, the two means were blended by fitting a single error function (spanning the eastward jet and corresponding to westward velocity) to the difference between the mean dynamic height and the mean SSH estimate. The relatively weak recircu-

lation gyres in the blended mean may be due to the missing barotropic component in the hydrographic data. This blended mean SSH retains the narrow jet structure in the vicinity of the Gulf Stream and allowed us to compute both the Gulf Stream position and the SSH difference across the jet.

Collinear height profiles for the 2.5-yr Geosat Exact Repeat Mission (November 1986–April 1989) were processed in a manner similar to that of the TOPEX/Poseidon data. However, an orbit correction was applied to the data (Caruso et al. 1990). Construction of the weekly SSH fields used for the Geosat data was described by Qiu and Kelly (1993); these maps were subsequently averaged to produce monthly fields on a  $0.5^\circ$  grid.

Other data fields available for the Geosat time period were used here (Caruso et al. 1995). Monthly net surface heat fluxes were estimated from the ECMWF values for September 1986–December 1989 on a  $1.125^\circ \times 1.125^\circ$  grid. Monthly sea surface temperature (SST) maps from the advanced very high resolution radiometer (AVHRR) were also used in analyses presented here. Mixed layer depths and temperatures were derived from values compiled by Levitus (1982).

### 3. Analysis of observations

#### a. Seasonal variations in SSH

Seasonal variations in both Geosat and TOPEX/Poseidon data were quantified using four measures: the position of the center of the jet, the SSH difference across the jet, the curvature of the jet, and the mean eastward geostrophic velocity. The SSH profiles along lines of constant longitude were first interpolated from the  $1^\circ$  grid to  $0.125^\circ$ , and the measures were computed at intervals of  $1^\circ$  long. For each measure an index was obtained by averaging over the specified longitude range (zonal average).

The SSH difference was estimated by fitting an error function to the SSH profile along each line of constant longitude, centered on the jet, in an approximation of “stream coordinates” (cf. Hall 1986), as opposed to on a fixed grid, such as that used by Zlotnicki (1991). Due to the narrow region over which the error function was fit, the surface transport index reflects the eastward flow of the Gulf Stream, rather than than the net flow (eastward minus recirculating flow). The position of the center of the jet was estimated using different methods for the TOPEX/Poseidon and the Geosat data, due to differences in the mean SSH field. For the Geosat data, the center of the jet was taken as the center of the error function. For the TOPEX/Poseidon data the latitude of the contours corresponding to  $-0.1$ ,  $0$ , and  $0.1$  m were averaged to produce a robust position estimate. The mean eastward velocity, analogous to the zonal index used for the jet stream, was computed by averaging

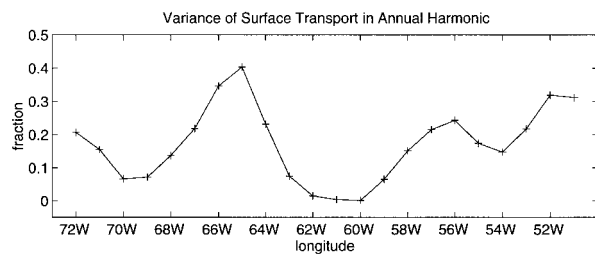


FIG. 3. Fraction of surface transport variance in the annual harmonic. The SSH difference across the Gulf Stream has no significant seasonal variation in the region  $59^{\circ}$ – $63^{\circ}$ W.

eastward velocity estimates  $0.5^{\circ}$  on either side of the peak jet velocity.

Curvature was computed from the following formula

$$\frac{1}{|R|} = \frac{|y''|}{[1 + y'^2]^{3/2}},$$

where  $y = f(x)$  is the position (latitude) of the jet center at the longitude corresponding to  $x$ ,  $y'$  and  $y''$  are the first and second derivatives of position with respect to the  $x$  coordinate, and  $R$  is the radius of curvature of  $y$ . The relatively coarse resolution of the SSH maps simplified the curvature calculations because there were no multiply valued positions at a given longitude, such as those observed in AVHRR images. Because these smooth maps may not accurately represent curvature statistics, additional statistics were computed on the anomalous positions of the centers of the jet using the original alongtrack SSH profiles. The position anomalies showed similar temporal variations to that in the curvature index (appendix A).

Based on an analysis of the strength of the seasonal cycle, the zonal indices described here were computed for two regions: an upstream region ( $73^{\circ}$ – $64^{\circ}$ W) and a downstream region ( $63^{\circ}$ – $50^{\circ}$ W). Figure 3 shows the fraction of surface transport variance described by a single annual harmonic as a function of longitude, using both Geosat and TOPEX/Poseidon data; two regions with significant seasonal cycles are separated by a region ( $59^{\circ}$ – $63^{\circ}$ W) with no significant seasonal cycle. Since the (eastward) seasonal transport varies greatly with longitude, regions with large seasonal variations presumably have compensating seasonal recirculating flows on either side of the Gulf Stream to conserve net transport in the stream. Although there were differences between the two altimeter time series (TOPEX/Poseidon indices have twice as much variance in the seasonal cycle as the Geosat indices), the upstream region consistently had a stronger seasonal cycle for both altimeter series (Table 1). In the downstream region the seasonal cycle was discernible only in the TOPEX/Poseidon indices of position and transport (Table 1).

There appears to be a distinct seasonal cycle of position and surface transport in the upstream indices for the TOPEX/Poseidon data (Fig. 4) and for the Geosat

TABLE 1. Annual cycle in position and surface transport.

Index	Upstream <sup>a</sup> % of variance	Downstream <sup>b</sup> % of variance
Position, TOPEX/Poseidon	70	69
Position, Geosat	32	7
Transport, TOPEX/Poseidon	72	24
Transport, Geosat	24	3

<sup>a</sup>  $73^{\circ}$ – $64^{\circ}$ W.

<sup>b</sup>  $63^{\circ}$ – $50^{\circ}$ W.

data (Fig. 5). Combining both series gives a fall (October) surface transport maximum corresponding to the most northerly positions, and a spring transport minimum corresponding to the most southerly positions. Based on a least squares fit of an annual harmonic to both the TOPEX/Poseidon and Geosat data (about 4 yr of data), the annual range in position in the upstream region is  $0.42^{\circ}$  lat and the annual range in the surface transport (fall minus spring) is 0.14 m. The curvature in TOPEX/Poseidon data appears to have a seasonal variation, with minimum curvature (straight path) in late summer (September). However, curvature from Geosat shows shorter timescales. The mean eastward velocity combines information about surface transport and meandering because meandering can increase the meridional velocity component and, therefore, decrease the eastward velocity without changing the transport. Mean eastward velocity, like curvature, also contains shorter timescales than the transport index.

#### b. Seasonal SSH and dynamic height variations

To determine whether the observed fall surface transport maximum is due to changes in the seasonal thermocline or to changes deeper in the water column, we compared the SSH fluctuations with the seasonal dynamic height variations from climatology. The winter/spring fields (February–April) were subtracted from the summer/fall fields (August–October, Fig. 6) for both the altimeter data and the dynamic height for several depth levels. To compensate for differences in spatial resolution, the altimetric SSH change in Fig. 6b was spatially smoothed. The dynamic height change for 0/1000 db (Fig. 6a) has a similar magnitude and sign to that of the altimetric fields (Fig. 6b) although the region of large positive values is considerably broader and noisier. The contribution to this 0/1000 db change is clearly dominated by the 0/250 db field (Fig. 6c); the dynamic height change for 250/1000 db (Fig. 6d) has the opposite sign (smaller dynamic heights in the fall than in the spring, south of the Gulf Stream). The similarity between the 0/250 db change and that from the altimeter suggests that the seasonal SSH is dominated by processes in the upper 250 m, in agreement with the results of Wang and Koblinsky (1996) using the recent Levitus climatology.

Much of the seasonal SSH variance is due to changes in the Gulf Stream position, as shown by a schematic

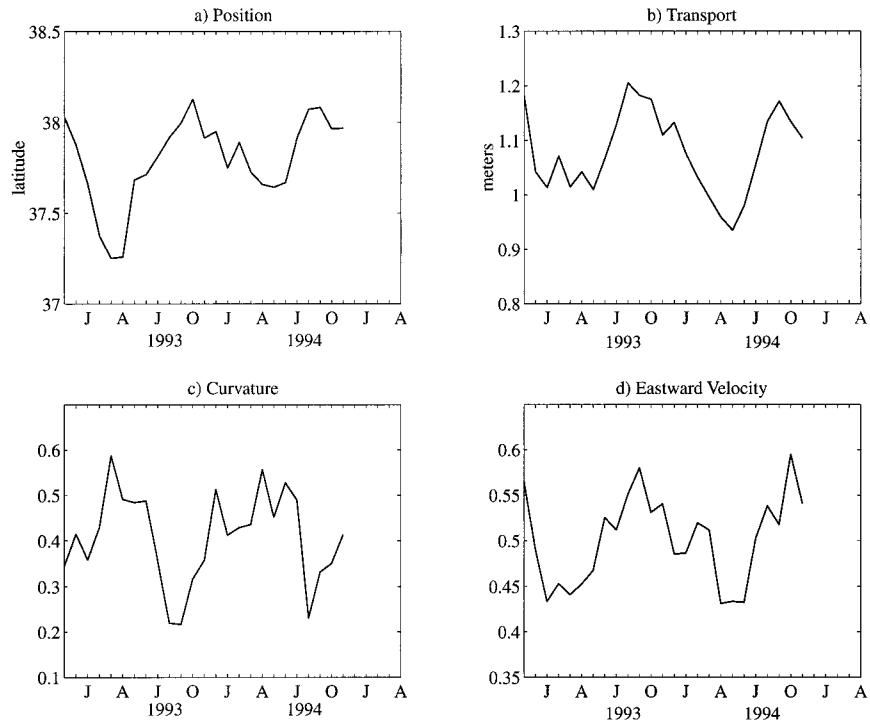


FIG. 4. Zonal indices for the upstream region from TOPEX/Poseidon. Longitudinally averaged indices for 73°–64°W for the Gulf Stream of (a) position, (b) SSH difference (surface transport), (c) curvature, and (d) eastward velocity. The first three indices show a clear seasonal cycle. SSH difference has a maximum in October, nearly coinciding with the most northerly position in September. Curvature has a minimum in August.

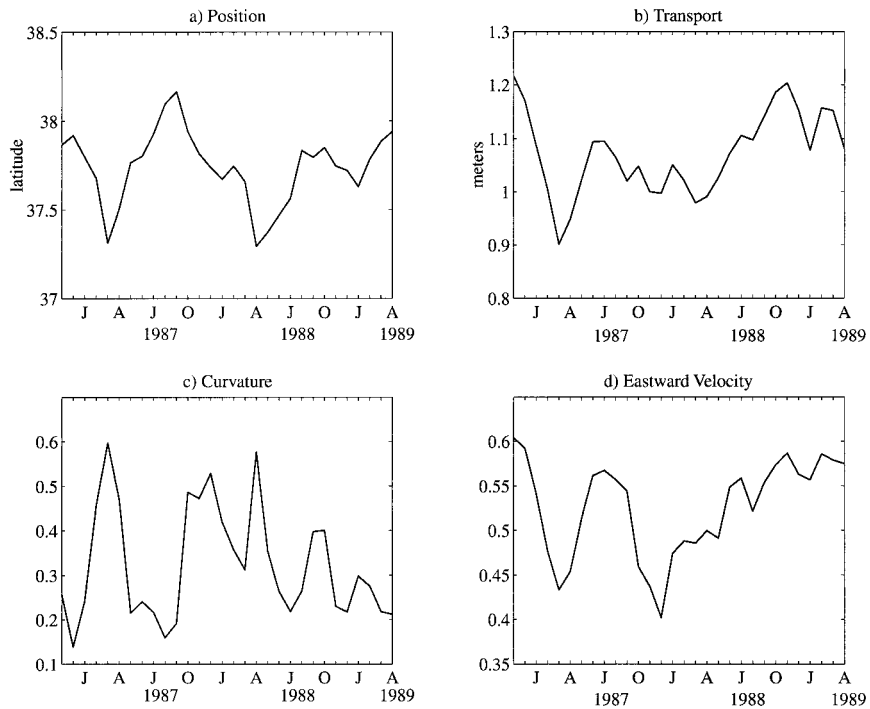
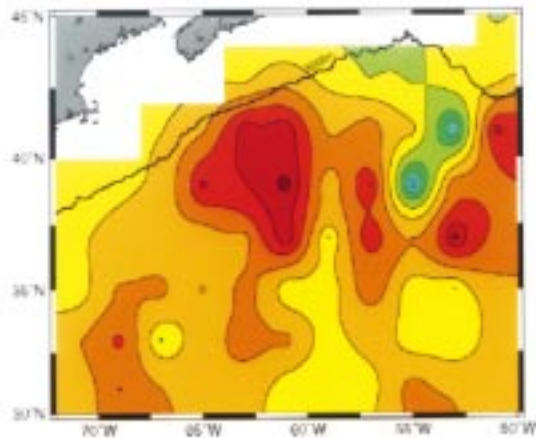
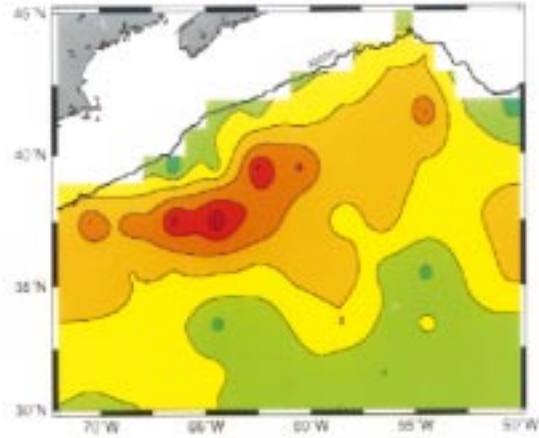


FIG. 5. As in Fig. 4 but from Geosat. The seasonal cycle is less apparent than for the indices from TOPEX/Poseidon SSH data in Fig. 4.

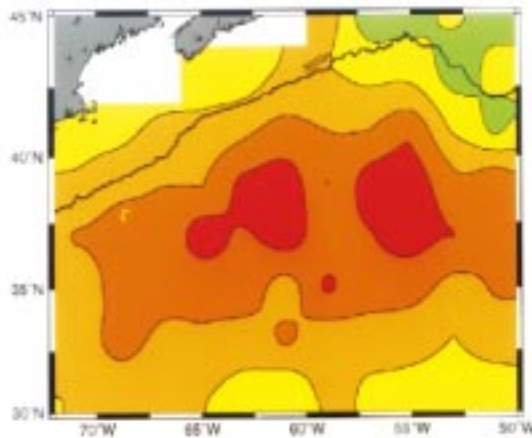
### Dynamic height differences (Fall minus spring)



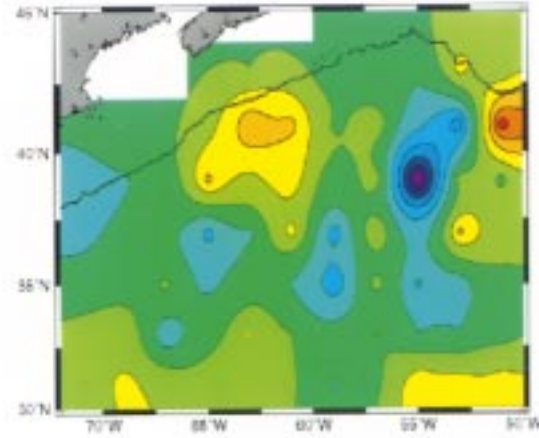
(a) LOC 0/1000 db



(b) Altimetric SSH



(c) LOC 0/250 db



(d) LOC 250/1000 db

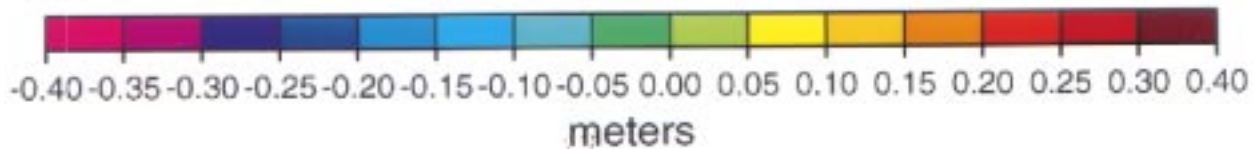


FIG. 6. Fall minus spring height change for (a) dynamic height of the surface relative to 1000 db, (b) SSH from a combination of TOPEX/Poseidon and Geosat data, and (c) dynamic height for the surface relative to 250 db and (d) for 250 db relative to 1000 db.

comparison of seasonal SSH profiles using fixed coordinates (Fig. 7a) and using stream coordinates (Fig. 7b). Although the surface transport may change seasonally by only a small amount (Fig. 7d), a small po-

sition change in a region with large SSH gradients produces a large seasonal change in SSH (Fig. 7c). The contribution to seasonal SSH changes (Fig. 8a) from position changes alone was estimated for each longitude

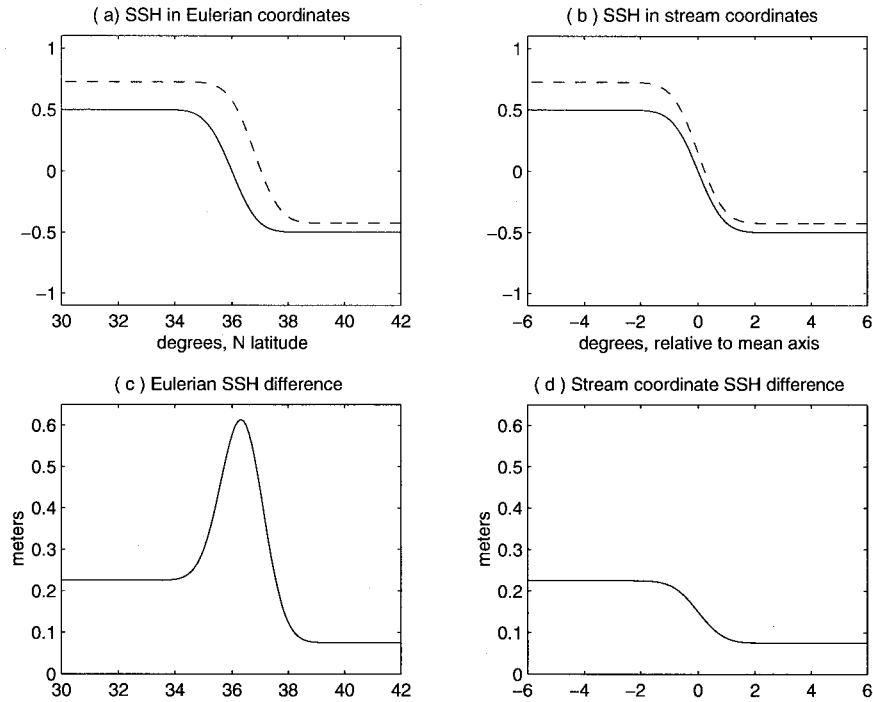


FIG. 7. Schematic of seasonal SSH changes in Eulerian and Lagrangian coordinates. Profiles of SSH across the Gulf Stream in (a) fixed coordinates and (b) stream coordinates for spring (solid line) and fall (dashed). SSH changes (fall minus spring) in (c) fixed coordinates and (d) stream coordinates.

by subtracting two error function profiles, each with the width and amplitude fixed at annually averaged values but one with the mean fall position and one with the mean spring position (Fig. 8b). The largest changes between the spring mean position (blue line in Fig. 8b) and the fall mean position (white line) correspond to the largest values of seasonal SSH change (Fig. 8a). In the region near  $63^{\circ}\text{W}$ , where the seasonal position excursion is largest, a seasonal SSH change of as much as 0.25 m is found due to position changes alone, compared with a total seasonal SSH change of about 0.35 m. Note that the position changes in Fig. 8b do not contribute to the SSH difference in the surface transport index (Figs. 4, 5), which is measured in stream coordinates, as discussed in section 2. However, the contribution from position changes is important in any analysis of SSH variations in Eulerian coordinates (fixed grid), as discussed in the next section.

The negative values of dynamic height change (fall minus spring, Fig. 6d) suggest that the spring transport below 250 m is a maximum. To determine the seasonality of the transport of the Gulf Stream, we computed the transport from the surface to the bottom of the water column at  $68^{\circ}\text{W}$  between  $36^{\circ}$  and  $41^{\circ}\text{N}$  from the LOC database. The volume transport in the spring exceeds the fall transport by about 7 Sv ( $\text{Sv} \equiv 10^6 \text{ m}^3 \text{ s}^{-1}$ ), or about 9% of the average transport (81 Sv), compared with a seasonal range of 8 Sv found by Sato and Rossby (1995).

### c. Seasonal heating and SSH variations

Based on the comparisons with hydrographic data, the observed seasonal SSH variations correspond to steric changes in the upper few hundred meters of the water column; we next wish to determine whether these steric changes can be explained by the ocean's response to net surface heat fluxes. An equation for steric changes in SSH can be obtained by combining the equation for thermal expansion (3) with the mixed layer heat equation,

$$\frac{\partial T_m}{\partial t} = \frac{Q_{\text{net}} - q(-h_m)}{c_p \rho_0 h_m} - \frac{\Delta T w_e}{h_m} - \mathbf{u} \cdot \nabla T_m + A_T \nabla^2 T_m, \quad (4)$$

where  $T_m(h_m)$  is the mixed layer temperature (depth) and  $\mathbf{u}$  is the velocity in the mixed layer (Qiu and Kelly 1993), to obtain

$$\frac{\partial \eta}{\partial t} = \alpha_T \left[ \frac{Q_{\text{net}}}{c_p \rho_0} - h_m \mathbf{u} \cdot \nabla T_m + A_T h_m \nabla^2 T_m \right]. \quad (5)$$

We have neglected vertical entrainment and heat losses out the bottom of the mixed layer  $q(-h_m)$  because these processes merely redistribute heat within the water column and do not change the heat content. We have assumed that the coefficient of thermal expansion  $\alpha_T$  is a function only of mixed layer temperature and that the largest contributions to SSH from advection and diffusion are in the mixed layer. If we neglect advection

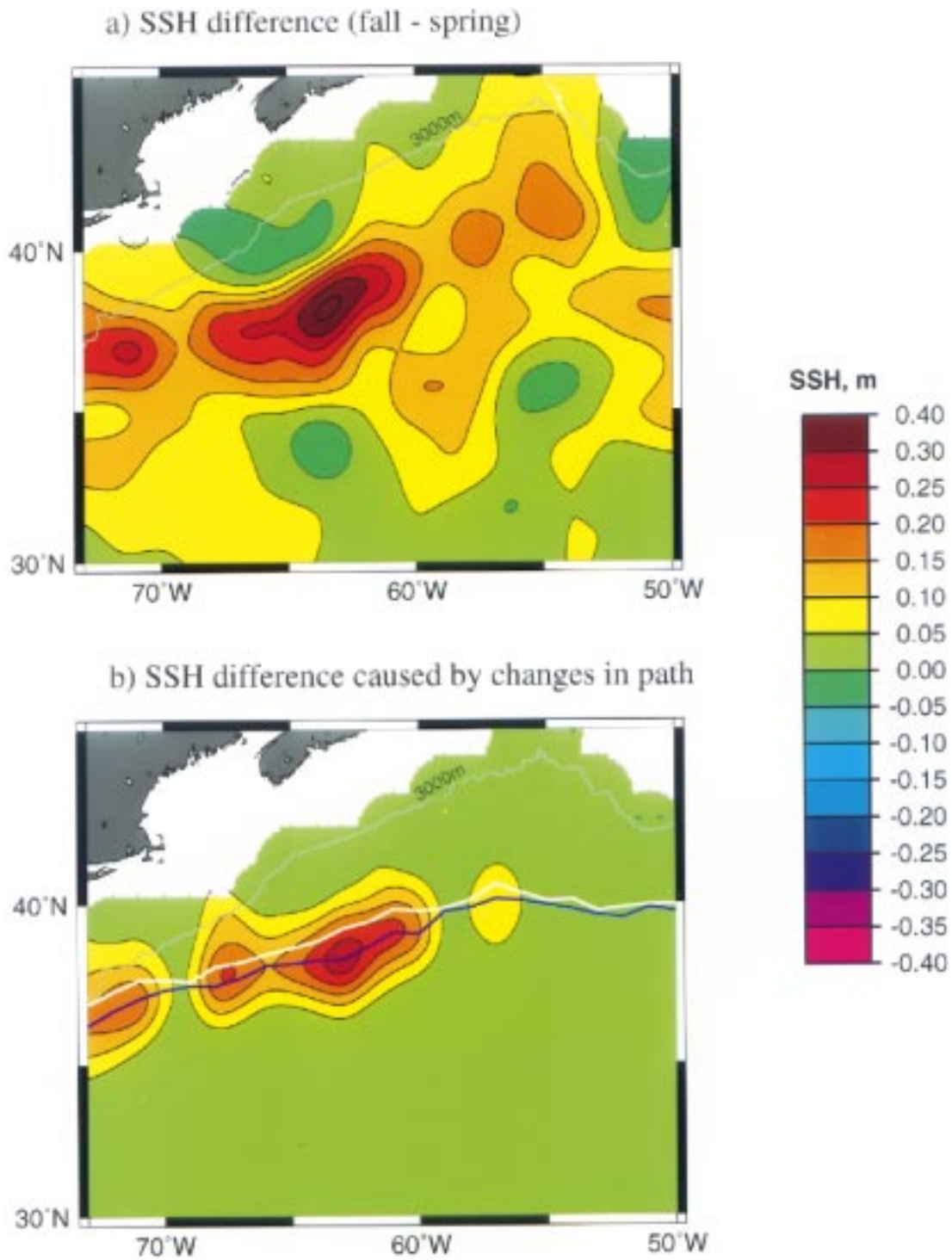


FIG. 8. The effect of position changes on seasonal SSH variations. SSH change (fall minus spring) for (a) the altimeter data and (b) the estimated contribution from position changes alone. The blue (white) line corresponds to the mean spring (fall) position of the Gulf Stream.

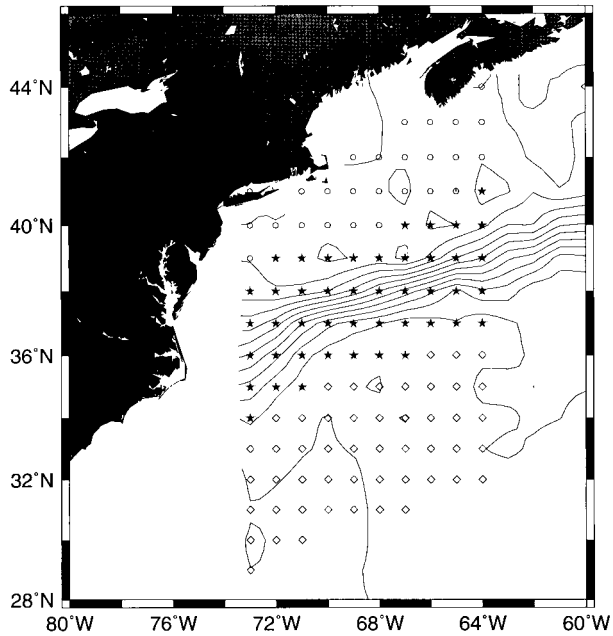


FIG. 9. Fixed grid points used to compute various quantities north of the Gulf Stream (open circles), within the Gulf Stream (stars), and south of the Gulf Stream (diamonds). The three regions were selected using contours of the mean SSH shown in light solid lines.

and diffusion, the expected steric anomaly can be computed simply as

$$\eta_{\text{steric}} = \int_t \frac{\alpha_T Q_{\text{net}}(t')}{c_p \rho_0} dt'. \quad (6)$$

To estimate the steric component of SSH, we used (6) and monthly heat fluxes  $Q_{\text{net}}$  derived from ECMWF values for 1987–88, a period for which SST and an estimate of the contribution of advection were also available (Kelly and Qiu 1995, hereafter KQ). However, we compared the results with monthly SSH variations derived from TOPEX/Poseidon data (1993–94), which had more accurate low-frequency variations than the Geosat data. For the analyses described below, the monthly values of all the variables were computed by averaging two years of data and then detrending the result. Monthly values for the coefficient of thermal expansion,  $\alpha_T$ , were estimated from the monthly AVHRR temperatures and a Taylor's expansion of the nonlinear equation of state. All of the comparisons were done on a fixed grid (Fig. 9) and were averaged over the three regions denoted by the symbols.

The agreement between the observed SSH and the estimated steric response for the regions north and south of the Gulf Stream is quite good (Figs. 10a and 10c). North of the Gulf Stream agreement in the phases is

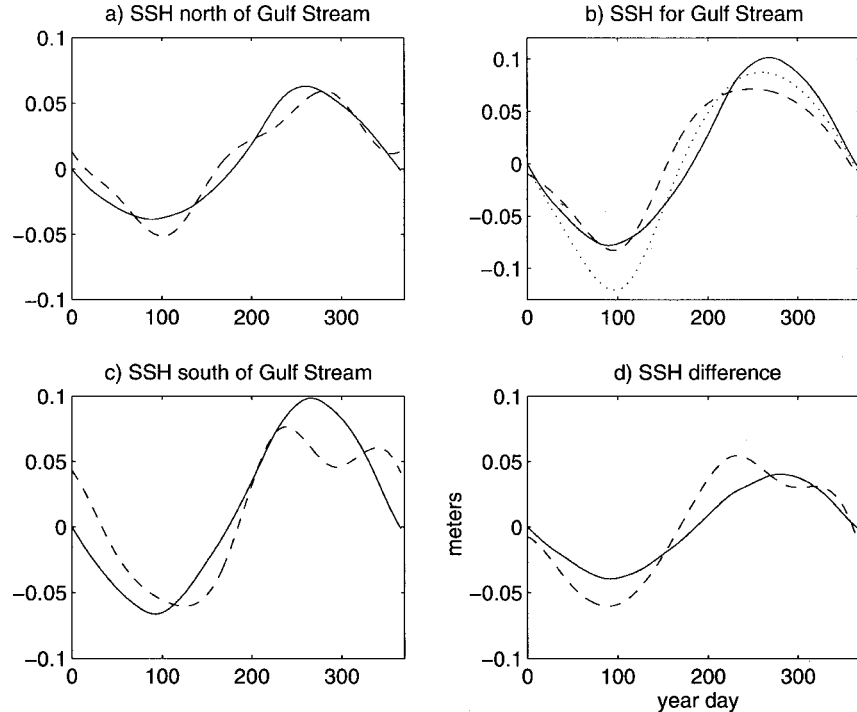


FIG. 10. Seasonal variations of SSH from TOPEX/Poseidon data (dashed line) and estimated using ECMWF net surface heat fluxes (solid line) for (a) the region north of the Gulf Stream, (b) the Gulf Stream itself, and (c) the region south of the Gulf Stream. (d) The SSH difference between the Gulf Stream region and the region to the north. In the Gulf Stream region (c), the residual SSH (dash) was calculated by subtracting an estimate of the SSH due to the variations in Gulf Stream position from the total seasonal variation of SSH (dotted).

also good (Fig. 10a), but south of the Gulf Stream there are some rather distinct discrepancies, particularly in the fall (Fig. 10c). Within the Gulf Stream region (Fig. 10b) the seasonal range of the steric response (solid line) is approximately 0.17 m, which is considerably less than the seasonal range of 0.22 m for the observed SSH (dotted line). Using (6) the heat flux required to produce the additional 0.05 m rise in SSH over a 6-month period is approximately  $47 \text{ W m}^{-2}$ . Based on this comparison, seasonal variations in ECMWF heat fluxes are too small to account for the observed SSH changes, in agreement with the conclusions of Wang and Koblinsky (1996). However, this discrepancy can be eliminated if seasonal Gulf Stream position variations are accounted for, as discussed below.

The large negative heat fluxes over the Gulf Stream are due to the loss of heat by the warm core; thus, the flux minimum presumably migrates seasonally with the Gulf Stream itself. It is unlikely in this coupled system that the position changes are a direct result of thermal expansion, as in (6), although they may be tied indirectly to the seasonal heating cycle, as suggested by Worthington (1976). Therefore, to separate SSH changes due to Gulf Stream position from SSH changes due to heat content, the comparisons should be done in stream coordinates. However, the coarse ECMWF grid cannot resolve the half-degree spatial variations needed for this calculation. Instead, we removed an estimate of the SSH contributions from seasonal position changes, as in the previous section, which resulted in an annual range of SSH of 0.15 m (dashed line in Figure 10c), a better agreement with the 0.17-m steric estimate. Thus, ECMWF heat fluxes are consistent with the observed SSH differences (surface transport) in the Gulf Stream region. The discrepancy between the Eulerian and stream coordinate SSH in Fig. 10c is much smaller than suggested by the schematic in Fig. 7, which is only slightly exaggerated, because all the values have been averaged over the regions shown in Fig. 9.

An estimate of the steric height difference across the Gulf Stream  $\Delta\eta_{\text{steric}}$  agreed well with the observed SSH difference anomaly after removing position effects on SSH in the Gulf Stream (Fig. 10d). The discrepancy between the observed and estimated values is primarily due to a phase difference between the predicted and observed SSH in the Gulf Stream region (Fig. 10b). We investigate in the next section whether advection could cause such a phase shift. The success of the steric response to heat flux (6) in explaining seasonal variations in SSH suggests that the SSH difference across the Gulf Stream is a measure of the difference in heat content between the Gulf Stream and the slope water to the north. Heat content is a function of both the magnitude of the temperature anomaly and the depth to which it penetrates,  $h_m$ , as

$$H = \int_{-h_m}^0 T'_m dz. \quad (7)$$

A comparison of (7) with the definition of steric height (3) shows that the SSH difference anomaly  $\Delta\eta'$  is a measure of the difference in heat content, weighted by the coefficient of thermal expansion,  $\Delta\eta' = \Delta(\alpha_T H)$ .

Next, we examine the relationship between seasonal mixed-layer depth and SSH. The fall maximum in SSH across the Gulf Stream  $\Delta\eta'$  corresponds to a minimum in mixed-layer temperature difference  $\Delta T'_m$  (Fig. 11a). Thus, the fall maximum must be produced by differences in mixed layer depth or in the coefficient of thermal expansion, which was computed using constant typical salinities for regions north and south of the Gulf Stream front and monthly temperatures. We solved for depth estimates  $h_m$ , which gave steric height close to the observed SSH anomaly, while also minimizing the departure from a spatially uniform initial estimate of mixed layer depth  $h_0(t)$ . Specifically, we minimized

$$[\eta'_{\text{obs}} - h_m \alpha_T T'_m]^2 + w^2 [h_0 - h_m]^2,$$

where  $w$  is a weight factor. The weight factor was set to twice the average value of  $\alpha_T$  to make the two constraints have approximately the same importance in the depth estimate. SST was used for mixed layer temperature  $T_m$ . To get sensible results, it was necessary to temporally lag the SST by a month so that the minimum in the steric height estimate corresponded to the minimum in observed SSH. This one-month discrepancy is consistent with that found between the AVHRR temperatures and climatological SST by KQ in their heat budget estimates.

For consistency between the observed seasonal SSH, the steric response to heating, and the seasonal cycle of mixed layer temperature, the mixed layer depth must be much deeper in the Gulf Stream (200 m in the winter) than in the slope water to the north (about 100 m, Fig. 11b). Climatological mixed-layer estimates based on a density criterion (e.g., Lamb 1984) show values similar to those estimated here for both the Gulf Stream and the slope water. In contrast, mixed layer depths based on a temperature criterion alone, as used by Qiu and Kelly (1993), KQ, and Wang and Koblinsky (1996), give larger depths for the slope water than for the Gulf Stream. Using the same mixed layer depth for both regions would reverse the seasonal SSH difference (Fig. 11d, dashed line), consistent with the temperature difference. Thus, it is primarily the relatively deep Gulf Stream wintertime mixed layer that is responsible for the seasonal SSH difference: the wintertime heat loss from the deep Gulf Stream warm core, as described by Worthington (1976), causes a large contraction of the water column. For comparison, an estimate of the seasonal steric height using the same (time varying) value for  $\alpha_T$  for both regions, and differing mixed layer depths, nearly eliminates the seasonal cycle in SSH (Fig. 11d, solid line); this suggests that an accurate estimate of  $\alpha_T$  is essential to interpret SSH differences  $\Delta\eta'$  in terms of heat content differences.

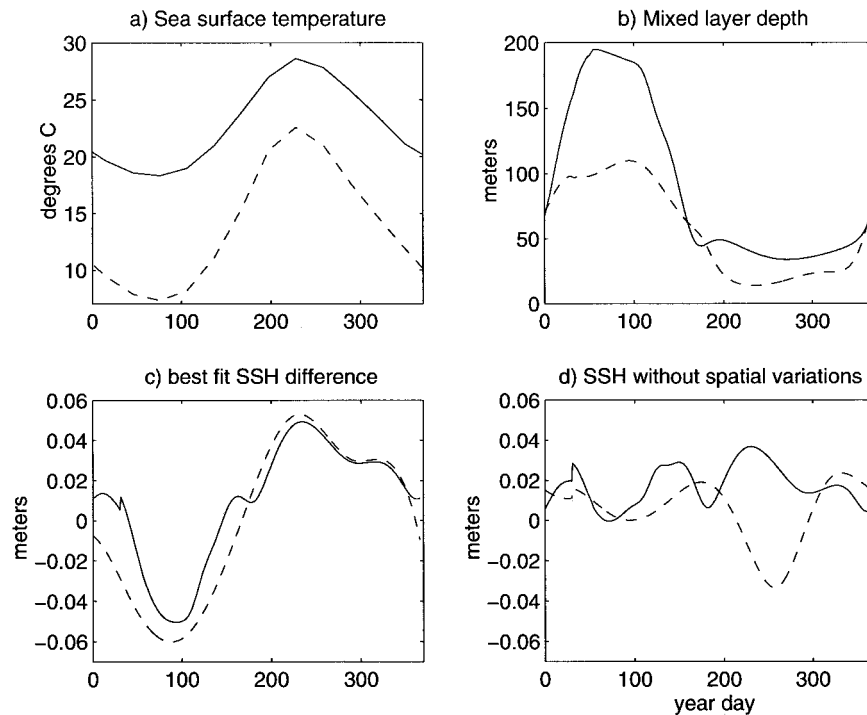


FIG. 11. The relationship between seasonal changes in SSH and mixed layer depth for (a) seasonal SST from AVHRR and (b) inferred mixed layer depth for the Gulf Stream (solid line) and the region to the north (dash). (c) Best-fit steric height and observed SSH (dash) and (d) SSH difference estimated using a constant coefficient of thermal expansion (solid) and a constant mixed layer depth (dash). The fall maximum in the SSH difference is primarily due to mixed layer depth differences across the Gulf Stream, but also to differences in the thermal expansion coefficient.

#### 4. Discussion

Based on 4 years of altimetric data, seasonal changes in the SSH of the Gulf Stream have been described using zonal indices and compared with hydrographic observations. The seasonal cycle is most pronounced west (upstream) of about  $63^{\circ}\text{W}$ , the region with a distinct warm core (Caruso et al. 1995). The combination of a more northerly position and a larger surface transport is directly analogous with the jet stream cycle, as described by Rossby (1939) and Namias (1950). As in the jet stream, the Gulf Stream index cycle is related to seasonal heating and cooling; however, the Gulf Stream surface transport maximum is confined to the upper few hundred meters of the water column. Although the 2-yr TOPEX/Poseidon record of “curvature” or meandering is suggestive of a seasonal cycle, a shorter period is apparent in the Geosat data, as noted by Kelly (1991). An analysis of a 7-yr record of Gulf Stream fronts from AVHRR by Lee and Cornillon (1995) showed a predominate 9-month period in meandering. In fact, the Geosat meandering peak values (Fig. 5) are remarkably similar to those of Lee and Cornillon for the same time period, despite the much coarser resolution of the altimetric data. Lee and Cornillon also showed that variations in meandering intensity are not related to larger-scale position variations. Therefore, the part of the jet

stream analogy governing meandering of the jet does not hold. Surface transport fluctuations with shorter timescales are probably related to Gulf Stream meanders. SSH differences across the Gulf Stream with amplitudes of 0.10–0.40 m at the temporal resolution of the Geosat altimeter (17 days) have been shown to be correlated with thermocline fluctuations (Kelly and Watts 1994). For comparison, seasonal variations in SSH difference have amplitudes of about 0.14 m, as described in section 3.

Seasonal surface transport variations from  $73^{\circ}$  to  $63^{\circ}\text{W}$  can be explained primarily as a response to seasonal heating using the net surface heat flux from ECMWF (averaged over a band  $4^{\circ}$ – $5^{\circ}$  wide). Our result differs from that obtained by Wang and Koblinsky (1996), who suggested that spatial gradients in the ECMWF heat fluxes were too small, because we first removed the SSH variations due to the seasonal position changes of the Gulf Stream. Without this correction, the observed seasonal SSH difference (in Eulerian coordinates) is about 30% larger than the predicted steric response. Conversely, the observed stream coordinate SSH difference should give a stream coordinate estimate of the net surface heat fluxes. The stream coordinate SSH of the Gulf Stream core can be estimated as the sum of the SSH to the north (Fig. 10a), a region not

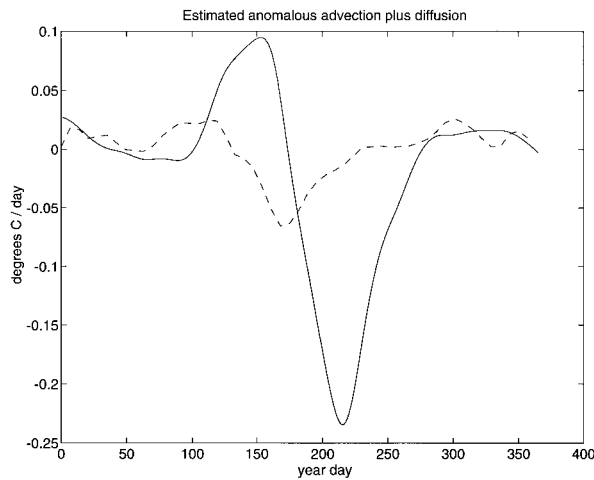


FIG. 12. The seasonal anomaly of advection and diffusion estimated from SSH. The difference between the steric height estimated from ECMWF heat fluxes and the observed SSH (solid), compared with the seasonal anomaly of advection and diffusion (dashed) from the heat budget estimates of Kelly and Qiu (1995). The seasonal SSH not explained by thermal expansion may be due to seasonal variations in advection and diffusion in the Gulf Stream.

affected by position changes, and the SSH difference in stream coordinates, estimated as described for the surface transport index in section 3. This gives an annual range of 0.26 m, larger by 50% than the 0.17-m value estimated from the ECMWF heat flux averaged over a band  $4^{\circ}$ – $5^{\circ}$  wide (Fig. 10b). Using (6), the surface heat flux in the Gulf Stream core should also have an annual range approximately 50% larger than the ECMWF Eulerian average; this would correspond roughly to wintertime values of  $-650 \text{ W m}^{-2}$  and summertime values of  $210 \text{ W m}^{-2}$ , compared with regional ECMWF averages in fixed coordinates of  $-431$  and  $140 \text{ W m}^{-2}$ , respectively, with all values zonally averaged in the region between  $73^{\circ}$  and  $63^{\circ}\text{W}$ .

There is a phase difference in the Gulf Stream region between the expected steric response and the observed SSH (Fig. 10b), which may be due to interannual variability between the time of the TOPEX/Poseidon data (1993–94) and the time of the heat flux estimates (1987–88) or to errors in the heat fluxes, which are difficult to quantify. Another possible explanation for the phase differences in the Gulf Stream region is seasonal variations in horizontal temperature advection and diffusion. From the residual between the observed SSH (Fig. 10b, dashed line) and the steric height (solid line), we can compute the corresponding temperature tendency residual as

$$\frac{\partial(\delta T_m)}{\partial t} = \frac{\partial(\delta \eta)}{\partial t} \frac{1}{h_m \alpha_T}$$

(Fig. 12, solid line) for comparison with the sum of the advection and diffusion terms (Fig. 12, dashed line) estimated by KQ. We see that the two estimates are qualitatively similar, although the KQ estimate is a fac-

tor of 3 smaller and leads the residual here by approximately 50 days. The seasonal variation in advection in KQ was due to a combination of early spring warming by the geostrophic Gulf Stream current and early summer cooling by the advection of cool slope water by the southward Ekman transport. In their analysis of the heat budget, Wang and Koblinsky (1996) neglected advection by Ekman transport, based on scaling the Ekman velocity component against the larger geostrophic velocity; however, KQ showed that advection by Ekman transport is actually more important than advection by geostrophic currents because the Ekman velocity is consistently oriented across the temperature gradient of the Gulf Stream, whereas the geostrophic velocity tends to be aligned with isotherms.

The ability to quantify interannual changes in the heat content of the Gulf Stream core may have important climate implications. Unlike SST, which in a shallow mixed layer can change rapidly in response to heat fluxes or to vertical entrainment, heat content is a temporally integrated measure of the heat input to the ocean; that is, it has a longer “memory” than SST. The warm core of the Gulf Stream supplies large quantities of heat to the atmosphere, particularly in the winter, because it is warmer than the surrounding ocean. The heat content of the Gulf Stream warm core, which is due to a combination of past heat input and advection, reflects the ability of the Gulf Stream to maintain this temperature gradient, despite cooling from winter storms.

There are some intriguing questions that cannot be answered by the above analyses. If seasonal heating is confined to the upper few hundred meters, why is there a seasonal cycle of position changes? Perhaps these seasonal position changes are surface-intensified. What is the connection between large-scale seasonal position changes, recirculation gyre changes, and seasonal meteorological forcing? The position variations may be related to changes in the recirculation gyres, which can be caused indirectly by cooling, or by fluctuations in the winds. Wintertime cooling can increase the strength of the Gulf Stream and its recirculation gyres by vertically mixing horizontal momentum downward into the water column (Huang 1990). This effect can be seen in the seasonal dynamic height variations that extend much further into the water column (Fig. 6d), associated with the subduction of mixed layer water and the formation of mode water. Perhaps this is a critical connection between seasonal heating and the Gulf Stream position.

## 5. Summary and conclusions

Zonally averaged indices of the Gulf Stream from four years of altimetric data show a seasonal cycle in the surface transport and position, similar to the zonal index cycle of the atmospheric jet stream. A maximum in the SSH difference across the Gulf Stream coincides with the most northerly position in the fall, with a minimum in the spring, consistent with previous observa-

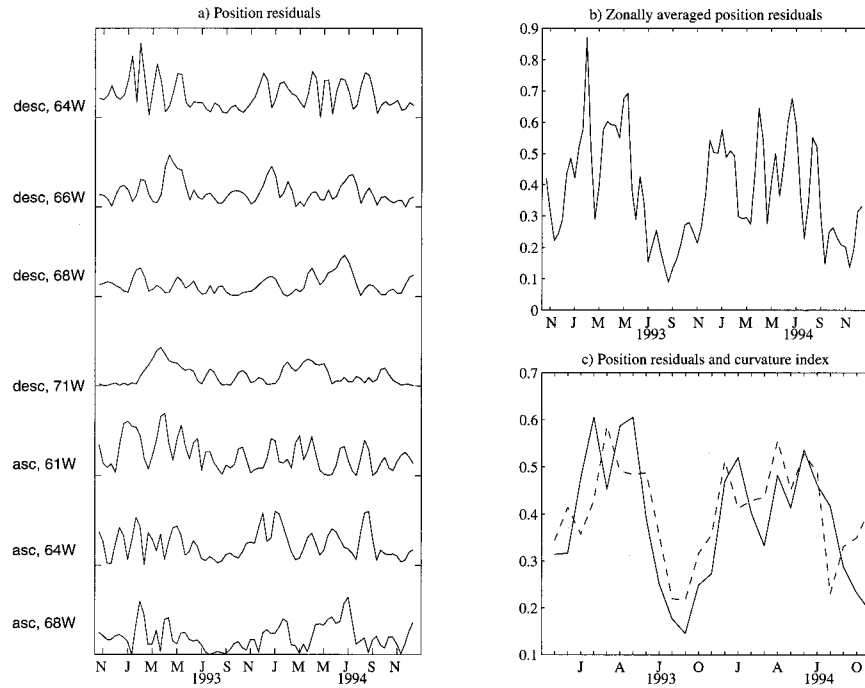


FIG. A1. Statistics of Gulf Stream position. (a) Position residuals from several ascending and descending TOPEX/Poseidon subtracks, with the longitude of the mean Gulf Stream position indicated. (b) Zonal average of the positions residuals in (a). (c) Temporally smoothed position residual index (dashed) and curvature index for the upstream region (solid, cf. Fig. 4c). As a check on the curvature index, which was derived from SSH maps on a coarse grid, position statistics were computed from the original along-track SSH data.

tions using only the Geosat altimeter; seasonal ranges in these parameters are 0.14 m for SSH difference and  $0.42^\circ$  lat for positions. The seasonal cycle is most pronounced west (upstream) of about  $63^\circ\text{W}$ .

Comparisons with hydrographic data suggest the observed fall maximum SSH difference is primarily from the upper few hundred meters of the water column. The spring volume transport exceeds the fall transport by about 7 Sv at  $68^\circ\text{W}$ .

The seasonal change in SSH from the TOPEX/Poseidon altimeter can be modeled successfully as a response to seasonal heating, using the net surface heat fluxes from ECMWF, if the SSH variations due to the seasonal position changes of the Gulf Stream are removed. A large discrepancy between the predicted steric changes and the SSH observations arises from using a fixed grid for an essentially Lagrangian process. Although they may be an indirect response to seasonal heating, seasonal position variations cannot be explained by thermal expansion. Seasonal variations in temperature advection and interannual variability may be responsible for smaller discrepancies.

*Acknowledgments.* The authors gratefully acknowledge the support of NASA under Contracts NAGW-1666 and NAGW-4806 (KAK and SS) and NAGW-4331 (RXH). The authors also benefited from discussions

with B. Qiu, M. Cronin, and G. Johnson. Comments from two anonymous reviewers greatly improved the text. TOPEX/Poseidon altimeter data were provided by AVISO and Geosat altimeter data were provided by NODC. ECMWF wind data and net surface surface heat flux were provided by NCAR.

## APPENDIX

### Estimates of Meandering from Gulf Stream Position

Because of the relatively coarse track spacing for TOPEX/Poseidon, the curvature index may not accurately reflect the presence of Gulf Stream meanders, which could lie between the tracks, or be aliased. As an additional check on the estimate of curvature, some simple statistics were computed on the positions of the centers of the Gulf Stream jet using SSH profiles from both the ascending and descending subtracks. For four descending and three ascending subtracks, which cross the mean Gulf Stream position at longitudes between  $61^\circ$  and  $71^\circ\text{W}$ , time series of position anomaly relative to the mean position for the two years, were computed (Fig. A1a). These anomalies show a tendency for smaller departures from the mean position for yeardays from about 160 to 300 (June–October) in 1993 and from about day

240 (August) in 1994. The root-mean-square departures (in degrees latitude) for all seven subtracks were computed and zonally averaged (Fig. A1b) to yield a regional estimate of position departures. This estimate, which has the original 10-day resolution, was then low-pass filtered for comparison with the curvature index, which was based on monthly SSH maps (Fig. A1c). The agreement between these two estimates suggests that the monthly SSH maps give sensible statistics for the meandering of the Gulf Stream.

## REFERENCES

- Caruso, M. J., P. J. Flament, Z. Sirkes, and M. K. Baker, 1990: Geosat processing tools for analyzing mesoscale ocean features. Tech. Rep. WHOI-90-45, Woods Hole Oceanogr. Inst., Woods Hole, MA, 200 pp. [Available from Woods Hole Oceanographic Institution, Woods Hole, MA 02543.]
- , S. Singh, K. A. Kelly, and B. Qiu, 1995: Monthly atmospheric and oceanographic surface fields for the western North Atlantic: October, 1986–April, 1989. Tech. Rep. WHOI-95-05, Woods Hole Oceanogr. Inst., Woods Hole, MA, 67 pp. [Available from Woods Hole Oceanographic Institution, Woods Hole, MA 02543.]
- Curry, R. G., 1996: HydroBase: A database of hydrographic stations and tools for climatological analysis. Tech. Rep. WHOI-Rep. 96-01, Woods Hole Oceanogr. Inst., Woods Hole, MA, 50 pp. [Available from Woods Hole Oceanographic Institution, Woods Hole, MA 02543.]
- Delworth, T., S. Manabe, and R. J. Stouffer, 1993: Interdecadal variations of the thermohaline circulation in a coupled ocean–atmosphere model. *J. Climate*, **6**, 1993–2011.
- Gill, A. E., and P. P. Niiler, 1973: The theory of seasonal variability in the ocean. *Deep-Sea Res.*, **20**, 141–177.
- Hall, M. M., 1986: Horizontal and vertical structure of the Gulf Stream velocity field at 68°W. *J. Phys. Oceanogr.*, **16**, 1814–1828.
- Hallock, Z. R., and W. J. Teague, 1993: Sea surface height fluctuations observed simultaneously with inverted echo sounders and Geosat. *J. Geophys. Res.*, **98**, 16 341–16 350.
- Huang, R. X., 1990: Does atmospheric cooling drive the Gulf Stream recirculation? *J. Phys. Oceanogr.*, **20**, 751–757.
- Kelly, K. A., 1991: The meandering Gulf Stream as seen by the Geosat altimeter: Surface transport, position and velocity variance from 73° to 46°W. *J. Geophys. Res.*, **96**, 16 721–16 738.
- , and S. T. Gille, 1990: Gulf Stream surface transport and statistics at 69°W from the Geosat altimeter. *J. Geophys. Res.*, **95**, 3149–3161.
- , and D. R. Watts, 1994: Monitoring Gulf Stream transport by radar altimeter and inverted echo sounders. *J. Phys. Oceanogr.*, **24**, 1080–1084.
- , and B. Qiu, 1995: Heat flux estimates for the North Atlantic. Part II: The upper ocean heat balance. *J. Phys. Oceanogr.*, **25**, 2361–2373.
- Lamb, P. J., 1984: On the mixed-layer climatology of the north and tropical Atlantic. *Tellus*, **36A**, 292–305.
- Lee, T., and P. Cornillon, 1995: Temporal variation of meandering intensity and domain-wide lateral oscillations of the Gulf Stream. *J. Geophys. Res.*, **100**, 13 603–13 613.
- Levitus, S., 1982: *Climatological Atlas of the World Ocean*. NOAA Prof. Paper No. 13, U.S. Govt. Printing Office, Washington, DC, 173 pp.
- , and T. Boyer, 1994: *World Ocean Atlas 1994*. Vol 4, *Temperature*. NOAA Atlas NESDIS 4, 117 pp.
- Lozier, M. S., W. B. Owens, and R. G. Curry, 1996: The climatology of the North Atlantic. *Progress in Oceanography*, Vol. 36, Pergamon, 1–44.
- Namias, J., 1950: The index cycle and its role in the general circulation. *J. Meteor.*, **7**, 130–139.
- Qiu, B., 1995: Variability and energetics of the Kuroshio Extension and its recirculation gyre from the two-year TOPEX mission. *J. Phys. Oceanogr.*, **25**, 1827–1842.
- , and K. A. Kelly, 1993: Upper-ocean heat balance in the Kuroshio Extension region. *J. Phys. Oceanogr.*, **23**, 2027–2041.
- , —, and T. M. Joyce, 1991: Mean circulation and variability of the Kuroshio Extension from Geosat altimetry data. *J. Geophys. Res.*, **96**, 18 491–18 507.
- Ray, R., B. Sanchez, and D. Cartwright, 1994: Some extensions to the response method of tidal analysis applied to the TOPEX/Poseidon altimetry (abstract). *Eos, Trans. Amer. Geophys. Union*, **75**, p. 108.
- Rosby, C.-G., 1939: Relations between variations in the intensity of the zonal circulation and the displacements of semipermanent centers of actions. *J. Mar. Res.*, **2**, 38–55.
- Sandwell, D. T., 1987: Biharmonic spline interpolation of GEOS-3 and Seasat altimeter data. *Geophys. Res. Lett.*, **14**, 139–142.
- Sato, O. T., and T. Rossby, 1995: Seasonal and low frequency variations in dynamic height anomaly and transport of the Gulf Stream. *Deep-Sea Res.*, **42**, 149–164.
- Singh, S., and K. A. Kelly, 1997: Monthly maps of sea surface height in the North Atlantic and zonal indices for the Gulf Stream using TOPEX/Poseidon altimeter data. Tech. Rep. WHOI-97-06, Woods Hole Oceanogr. Inst., Woods Hole, MA, 46 pp. [Available from Woods Hole Oceanographic Institution, Woods Hole, MA 02543.]
- Tai, C.-K., 1990: Estimating the surface transport of meandering oceanic jet streams from satellite altimetry: Surface transport estimates for the Gulf Stream and the Kuroshio Extension. *J. Phys. Oceanogr.*, **20**, 860–879.
- Teague, W. J., and Z. R. Hallock, 1990: Gulf Stream path analysis near the New England Seamounts. *J. Geophys. Res.*, **95**, 1647–1662.
- Tracey, K. L., and D. R. Watts, 1986: On Gulf Stream meander characteristics near Cape Hatteras. *J. Geophys. Res.*, **91**, 7587–7602.
- Wang, L., and C. J. Kobalinsky, 1995: Low-frequency variability in regions of the Kuroshio Extension and the Gulf Stream. *J. Geophys. Res.*, **100**, 18 313–18 331.
- , and —, 1996: Annual variability of the subtropical recirculations in the North Atlantic and the North Pacific: A TOPEX/Poseidon study. *J. Phys. Oceanogr.*, **26**, 2462–2479.
- Worthington, L. V., 1976: On the North Atlantic circulation. *Johns Hopkins Oceanogr. Stud.*, **6**, 110 pp.
- Zlotnicki, V., 1991: Sea level differences across the Gulf Stream and the Kuroshio Extension. *J. Phys. Oceanogr.*, **21**, 599–609.